Multiobjective optimization of skim milk microfiltration based on expert knowledge

Maëllis Belna, Amadou Ndiaye, Franck Taillandier, Christophe Fernandez, Louis Agabriel, Geneviève Gésan-Guiziou

Expert Systems With Applications 205 (2022) 117624

Contents lists available at ScienceDirect

Expert Systems With Applications

journal homepage: www.elsevier.com/locate/eswa

Multiobjective optimization of skim milk microfiltration based on expert knowledge

Maëllis Belna[a,b,c,*,1], Amadou Ndiaye[b], Franck Taillandier[d,*], Christophe Fernandez[b], Louis Agabriel[c], Geneviève Gésan-Guiziou[a]

[a] STLO, INRAE, Institut Agro, 35000 Rennes, France
[b] INRAE, Université de Bordeaux, I2M, 33400 Talence, France
[c] Boccard, Research and Development, 35360 Montauban-de-Bretagne, France
[d] INRAE, Aix-Marseille Université, RECOVER, France

ARTICLE INFO

Keywords:
Dairy sector
Expert knowledge
Microfiltration
Modelling
Multiobjective optimization
Real-world problem

ABSTRACT

Optimizing food processes is a complex task made harder by gaps in knowledge on process performance mechanisms, by the complexity inherent to the food product itself, and by the many heterogeneous variables involved in prediction models. Microfiltration of skim milk with a 0.1-µm pore-size membrane is a typical example (MF). MF is commonly used as a unit operation to separate the two major milk protein into valuable fractions for cheesemaking and food formulations. However, despite its importance for the dairy industry, the MF process has never been optimized to integrate conflicting stakeholder objectives such as maximizing quality of product outputs while minimizing cost inputs and addressing environmental impacts. This work addressed the multiobjective optimization of 0.1-µm skim milk MF by considering conflicting stakeholder-defined objectives and integrating expert and scientific knowledge into the formulation of the multiobjective problem. The multiobjective MF problem was modelled by considering the quality of product outputs, operating variables, process design and cost inputs, and using both scientific data and expert knowledge. Over a thousand Pareto-optimal solutions were found, including solutions close to current industry practice but also innovative new solutions. This work opens new perspectives for using multiobjective optimization techniques to design and optimize food processes.

1. Introduction

Crossflow microfiltration of skim milk (MF) with a 0.1-µm pore-size membrane is commonly used in the dairy industry as a unit operation to separate two main groups of proteins: native casein micelles (retentate fraction), which are used to make cheese, and milk serum proteins (permeate fraction), which are mainly used as ingredients to formulate food for specific populations (e.g. elderly people, infants) (Gésan-Guiziou et al. 1999; Saboya & Maubois, 2000; Brans et al. 2004). The rationale for this study stems from the fact milk MF today is still designed and run empirically based on the know-how of dairy processors and equipment manufacturers (Belna et al., 2020). All industrial MF process designs employ the same set of stages in order to simplify the sizing problem. This empirical approach makes it hard to define an optimization methodology via a scientific and therefore repeatable approach.

A multiobjective optimization process essentially requires three steps: formulation of the multiobjective problem, mathematical or algorithmic modelling of the objectives, and the optimization step itself. Formulating the multiobjective optimization problem for MF is a complex task, due to: i) the need to simultaneously consider the quality of product outputs (input milk, permeate fraction, retentate fraction), operating conditions, design, and cost input; ii) competing contradictory objectives, for example maximizing the milk serum protein recovery ratio while minimizing economic costs; iii) the large number of heterogeneous variables involved (ordinal, cardinal, discrete, continuous), and iv) the non-linearity of certain relations between variables and objectives (Belna et al., 2020). The formulation of the MF multiobjective

* Corresponding authors.
E-mail addresses: mbelna@boccard.fr (M. Belna), amadou.ndiaye@free.fr (A. Ndiaye), franck.taillandier@inrae.fr (F. Taillandier), christophe.fernandez@inrae.fr (C. Fernandez), lagabriel@boccard.fr (L. Agabriel), Genevieve.gesan-guiziou@inrae.fr (G. Gésan-Guiziou).
[1] ORCID: https://orcid.org/0000-0002-8180-8225.

https://doi.org/10.1016/j.eswa.2022.117624
Received 20 October 2021; Received in revised form 17 February 2022; Accepted 17 May 2022
Available online 29 May 2022

problem—from definition of the problem to identification of the decision variables, objectives, and their influential relations—has already been achieved in Belna et al. (2020). The remaining obstacle to multiobjective optimization is to model the optimization objectives. However, modelling the objectives in terms of decisions on optimal membrane type, operating variables, process design, economic costs and product characteristics is a complex task made harder by the lack of predictive MF performance models. This lack of appropriate models stems from a lack of knowledge on the mechanisms involved in the MF process (Jimenez-Lopez et al., 2008; Tolkach & Kulozik, 2006) and the complexity inherent to the allied products (milk, retentate fraction and permeate fraction). In order to translate the relationships between MF system variables and optimization objectives mathematically or algorithmically, it is necessary to collect and collate the existing knowledge and generate any missing knowledge. This knowledge can come from various different sources, such as extant literature, pilot-scale laboratory data, industrial production runs, or experts.

Coupling knowledge integration and optimization is an interesting strategy for solving multiobjective problems in a field where the available knowledge is incomplete (Hobballah et al., 2018). In order to describe the influential relations between variables and optimization objectives, practitioners usually employ scientific experiments. However, if the body of experimental work is too substantial and expert knowledge is available, then knowledge can be gathered from experts. By asking experts about their knowledge on a specific scientific phenomenon, it is possible to define the influential relations between the variables describing that phenomenon. In recent years, two studies have used this integration of expert knowledge to model food processes. The first combined expert knowledge and rheological data on French bread to predict state of the dough and bread based on key characteristics of the raw materials and processing conditions (Ndiaye et al., 2009a). The second predicted cheese ripening based on from biochemical measurements and sensory observations of its characteristics as a function of the temperature and relative humidity of the ripening chamber (Baudrit et al., 2010; Sicard et al., 2011). To our knowledge, only Hobballah et al. (2018) has developed a method to integrate expert knowledge into the formulation of a multiobjective problem. This formulation method, developed for the design of wood fibre-based thermal insulation, was recently transposed and adapted to the food process of the 0.1-µm skim milk microfiltration (Belna et al, 2020). However, it remains to be demonstrated whether this approach can also serve to model the optimization objectives and the implementation of the full multiobjective optimization.

To address this goal, this study set out to model the objectives and solve the MF multiobjective problem by coupling the integration of expert and knowledge and scientific data with multiobjective optimization techniques.

2. Background

2.1. Milk microfiltration: Principle and main operating variables

MF is a membrane operation that separates casein micelles from serum proteins to reach a volume reduction ratio (*VRR*) equal to 3. This *VRR*, defined as the ratio of feed flow rate (Q_{feed}) to retentate extraction flow rate (Q_r), makes it possible to adjust the target concentration of casein micelles in the retentate fraction.

It has been already demonstrated that a high crossflow velocity (v) (~7 m.s^{-1} for ceramic membranes) at low (<1 bar) transmembrane pressure (*TMP*) results in high MF performances, i.e. high permeation flux (the mass flux that permeates through the membrane, *Jp*) and high serum protein transmissions (*TrSP*) (Le Berre & Daufin, 1996; Gésan-Guiziou et al., 1999; Jimenez-Lopez et al., 2008; Tremblay-Marchand et al., 2016; Heidebrecht et al., 2018). The crossflow velocity is set up to create friction and minimize the accumulation of trapped proteins and fouling at the membrane surface. *TMP*, defined as the pressure difference between retentate side and permeate side, is the driving force of the operation, and it forces the permeate to pass through the membrane. The transmission ratio of serum proteins characterizes the ability of the membrane to let the serum proteins pass through. However, high crossflow velocities induce high pressure drops and are not generally compatible with low *TMP*. In order to simultaneously apply a high crossflow velocity and a low *TMP*), microfiltration needs to be carried out with specific membrane technologies.

Skim milk MF can use either ceramic or polymeric spiral-wound membranes, with three different types of membrane technologies. It can be carried out with ceramic membranes using the uniform transmembrane pressure (UTP) system (Sandblöm, 1974), which can maintain a low and even TMP throughout the length of the membrane by circulating permeate in co-current mode to retentate. Even though the UTP system offers very good performance and has enabled the emergence of industrial-scale MF (Le Berre & Daufin, 1996; Gésan-Guiziou et al., 1999), it still has major drawbacks. It has very high energy consumption and investment costs, as permeate circulation requires an additional pump on the permeate side. In the 2000s, two alternatives were proposed to make MF more economically attractive. The first alternative eliminates the need for the permeate-side pump by using innovative ceramic membranes called permeability gradient membranes (GP® and Isoflux®) (Garcera & Toujas, 1998; Skrzypek & Burger, 2010). These membranes make it possible to vary the permeability (and hydraulic resistance) properties between the inlet and outlet of the membranes, to compensate for TMP gradients. However, these ceramic membranes are designed to work with a predefined retentate pressure drop in order to deliver good filtration performances in terms of permeation flux and serum protein transmissions, which makes them ill-adapted to all the operating conditions sought by the industry. The second alternative is polymeric spiral-wound microfiltration membranes (SW). These polymeric membranes have a more cost-competitive but offer lower filtration performances (Lawrence et al., 2008). Each type of membrane thus has its own expected performances (Table 1), which leads to conflicting objectives. Designing and conducting MF in an optimal way thus requires a multiobjective optimization process to find a compromise.

This study considered three membrane technologies for MF: i) a 0.1-µm ceramic UTP tubular membrane, i.e. Pall 7P1940 UTP (19 channels, 4-mm diameter, 1.68 m^2 filtration area); ii) a 0.1-µm ceramic GP® tubular membrane, i.e. Pall 7P1940 GP (19 channels, 4-mm diameter, 1.68 m^2 filtration area); and iii) an 800-kDa polymeric spiral wound (SW) membrane, i.e. Synder FR 3A 6338 (46-mil spacers, 15.9 m^2 filtration area). These three membranes are widely used in industry, and termed “ceramic UTP”, “ceramic GP” and “polymeric SW”, respectively,

Table 1
Order-of-magnitude performances of the membrane technologies for a volume reduction ratio of 3 and depending on operating conditions.

Performance	Ceramic UTP	Ceramic GP	Polymeric SW
Filtration temperature (°C)	50	50	8–12
Permeation flux (L.h^{-1}.m^{-2})	75–100	75	10
Serum protein transmissions (%)	65–70	60	20–50
Membrane costs (€)*	High	Very high	Very low
Membrane lifetime (years)	10	10	2–3
Production schedule for 24 h	2 × 8 h runs + 2 cleaning and disinfection steps	2 × 8 h runs + 2 cleaning and disinfection steps	At 12 °C, 1 × 20 h run + 1 cleaning and disinfection step

*Confidential.

in this paper.

The full description of the MF optimization framework can be found in Belna et al., (2020). In a first approach, the assumptions and choices made were intended to simplify the multiobjective problem (Table 2). Additional assumptions were then made during subsequent data acquisition and modelling, especially for the models used to design the process.

Table 2
Assumptions and choices made in the MF optimization framework.

Hypothesis	Description
Milk history and pre-treatment	Bovine milk was stored at 4 °C for 48 h, skimmed, thermized (at 68 °C for 30 s), and bactofuged to decrease the bacterial count of the processed milk. In order to reach mineral equilibria prior to filtration, the skim milk was held at filtration temperature for 20 min. Pre-treatments and storage conditions were set as constants.
Filtration temperature	The temperature was set to the routine MF temperature, i.e., 50 °C for ceramic GP and ceramic UTP, and 12 °C for polymeric SW.
Transmembrane pressure	Transmembrane pressure was constant and similar at each stage of the MF process.
Geometrical description of MF stages	The MF plant was described geometrically, with *n* the number of stages, *i* the i[th] line in parallel in one stage, and *j* the j[th] module on line *i*. For a given stage, there was the same number of modules on each line *i*.
Module description	The module is composed of only 19 membranes for ceramic UTP, 37 membranes for ceramic GP, and one membrane for polymeric SW. All these configurations are classically used in the industry.
Retentate recirculation flowrate	Retentate recirculation flow (Q_{rec}) was expressed as an equivalent to a 7-membrane module for ceramic membranes and to a single-membrane module for polymeric membranes.
Volume reduction ratio, VRR	VRR values were limited to values up to 3.0 in this study, whereas industrial installations can reach values of up to 3.5.
Diafiltration	In this study, the MF system is performed in continuous mode without diafiltration. During diafiltration, adding a solvent increases the recovery of serum protein in the permeate, which therefore becomes more diluted. Adding solvent increases the volume of the MF permeate fraction, which influences the design of the ultrafiltration process (upstream of the MF). Ultrafiltration process design is outside the scope of this study.
Casein permeation	In this study, we do not consider casein permeation and we make no distinction between casein micelles and free caseins. There is scarce data on casein permeation as function of influence parameter (filtration temperature, concentration factor, membrane type and diafiltration mode (ratio and solvent)) in the literature (Zulewska and Barbano, 2013; Zulewska et al., 2009; Beckman & Barbano, 2013; Hartinger & Kulozik, 2020) and none of it is relevant for the three filtration technologies studied here.
Cleaning and disinfection considerations	Cleaning and disinfection procedures were defined according to industrial standards and assumed to be effective and reproducible for each type of membrane. Consequently, water flux was assumed to be constant, and chemical degradation of the membranes was assumed to be negligible throughout their lifetime.
Investment costs	The investment cost was calculated from:Cost of equipment (i.e., tanks, pumps, heat-exchangers, membranes, modules, sensors, plant automation and cleaning plant) .Cost of the hours worked by people involved in the conception and commissioning of the MF process (i.e., engineering department, project follow-up, installation and commissioning, automation programming).
Production costs	Production cost was estimated from water, energy and chemicals consumption and maintenance and membrane replacement costs.

2.2. Formulation of the multiobjective problem

The multiobjective problem is generally defined as a set of k conflicting objectives: to be optimized subject to m constraints, where objectives and constraints are defined according to a set of n decision variables (Hwang & Masud, 1979; Ndiaye et al,. 2009b):

$$\text{Optimize.} \vec{f}(\vec{x}) = [f_1(\vec{x}), f_2(\vec{x}), \cdots, f_k(\vec{x})]$$

$$\text{subject to } g_j(\vec{x}) \leq 0 \; for \; j = 1, \cdots, p \text{ and } h_j(\vec{x}) = 0 \; for \; j = p+1, \cdots, m \tag{1}$$

where $\vec{x} = (x_1, x_2, \cdots, x_n)$ is the vector of decision variables, $f_i(\vec{x}) \; for \; i = 1, \cdots, k$ are the objective functions, and $g_j(\vec{x})$ and $h_j(\vec{x})$ are the inequality and equality constraints, respectively, of the problem.

Solving a multiobjective optimization problem with conflicting objectives consists in identifying Pareto-optimal compromises. A compromise is Pareto-optimal if it is Pareto-dominant (Deb, 1999; Van Veldhuizen and Lamont, 2000; Reyes-Sierra & Coello Coello, 2006; Ndiaye et al,. 2009b), i.e., any improvement in one objective degrades at least one other objective. The Pareto-optimal compromises, which are a set of optimal but non-equivalent solutions, are located on a front named Pareto front. The Pareto front can serve to choose of an optimal solution in terms of accommodating decisionmaker preferences (technical, economical, etc). The Pareto dominance can be defined as:

$\vec{x} = (x_1, \cdots, x_n)$ is said to dominate $\vec{x'} = (x'_1, \cdots, x'_n)$ (written $\vec{x} \prec \vec{x'}$) if and only if $\forall i \in \{1, \cdots, n\}, \; x_i \leq x'_i$ and.$\exists \; j \in \{1, \cdots, n\}, \; x_j < x'_j$

The first step in the effort to optimize skim milk MF is to formulate the multiobjective problem, which was carried out by Belna et al. (2020). In this first step, the relevant optimization objectives and experts were chosen. The necessary knowledge domains were identified, evaluated using a scoping matrix, and rated according to two criteria Belna et al. (2020): the relative importance of capturing knowledge from the domain, and the ease of capturing knowledge from the domain (Milton, 2007). First, knowledge was collected using semi-structured interviews in each knowledge domain to identify the pertinent variables and their relations (Cooke, 1994) and the allied influence relations. Then, the influence relations extracted from interview transcripts were represented as causal maps that represent the relations between decision variables and optimization objectives, including the necessary intermediate variables (Montibeller & Belton, 2006). Finally, maps of collected knowledge were constructed and merged. The outcome of this process was five objectives chosen: maximize the casein concentration in the retentate fraction (CD_{CNr}, referred to hereafter as *retentate concentration*), maximize the serum protein concentration in the permeate fraction (CD_{SPp}, called *permeate concentration*), maximize the serum protein recovery ratio in the permeate fraction (η_p, called *permeate recovery*), minimize the investment cost (*CI*), and minimize the production cost (*CPR*). The MF problem was formulated using this selection of optimization objectives. The experts did not consider environmental impacts as an optimization objective but more as a decision criterion on the different Pareto-optimal solutions. In this work, a part of the environmental impact is considered through the production costs, i.e., water, vapor and electricity consumption rates.

In the food domain, metaheuristics are mainly used to solve multiobjective problems for operations such as drying (Vitor & Gomes, 2011; Janaszek-Mankowska, 2018), frying (Amiryousefi et al., 2014) or heat exchangers (Deka & Datta, 2017; Janaszek-Mankowska, 2018). The scholarship has used two main metaheuristics: the non-dominated sorting genetic algorithm-II (NSGA-II) (Deb et al., 2002), and particle swarm optimization (PSO) (Kennedy & Eberhart, 1995). Following the "no free lunch theorem" (Wolpert & Macready, 1997) where there is no algorithm better than all the others for any optimization problem, NSGA-II was used in this study. NSGA-II is a robust and widely-used metaheuristic that is recognized as one of the most efficient evolutionary multiobjective algorithms (Yusoff et al., 2011), and it can be freely implemented in various open-sources multiobjective optimization frameworks.

3. Modelling the optimization objectives

3.1. Methodology for modelling the optimization objectives

In order to solve the multiobjective problem of MF optimization, it was necessary to formalize the optimization objectives through mathematical equations or algorithms. The literature already contains some influence relations, such as Darcy's law describing the influence relations between permeation flux, transmembrane pressure, filtration resistance and permeate viscosity. However, several relationships between variables were not described in the literature and needed to be modelled in this work. Ideally, experiments should be done to obtain data for modelling these influence relations, which makes it possible to simultaneously account for the variance in the variables of the same dataset and their reliability through a necessary and sufficient number of repetitions. However, this may require a large number of experiments to combine all the operating conditions for each influence relation that needs to be described. Here, for the sake of pragmatism, the influence relations between variables were essentially modelled based on existing data that has been obtained in experiments conducted over the past few years. The objective of the modelling step was to define the equations of the optimization objectives and made them sufficiently representative of the MF system over the ranges of variation in the existing data. This strongly constrained the domain of validity of the optimization objective equations since the data available did not cover the whole validity domain of the MF system. The technical objectives of the MF (retentate concentration, permeate concentration, permeate recovery) can be evaluated via experimental research, which is not the case for the economic cost objectives. We therefore had to mobilize two different strategies for building the equations of the optimization objectives. For each influence relation, the modelling was done based on either a published equation, an experimental dataset, or expert knowledge (Fig. 1). Some of the existing datasets had to be completed by further trials to make them robust enough for mathematical modelling. When there were no existing equations and further experimental trials were impossible, we used expert knowledge to formalize the influence relation. The formalization of the influence relation was either quantitative or qualitative.

A second strategy was implemented to estimate the objectives of minimizing investment and production costs. The approach mobilized was to start from an existing installation and to break it down into functional blocks (upstream environment, feed and retentate areas, permeate area, stages, downstream environment, and cleaning and disinfection area) in order to retrieve the purchase price. A benchmark industrial unit was chosen for each of the different membrane types, and each MF unit was broken down into functional blocks. The cost of each functional block was determined from equipment cost databases, from consultation with suppliers when the data available was not consistent enough, and from expert knowledge in cases where no data was available (Fig. 2). The functional blocks were used to evaluate the investment cost of other MF units to validate the methodology. This strategy was carried out using expert knowledge with additional data from equipment suppliers.

Multiple linear regressions made it possible to build models that were sufficiently representative for the MF optimization objectives. These models have an R^2 between 0.71 and 0.99, and more than 60% of the objective equations have an R^2 higher than 0.85. The set of influence relations was modelled using a combination of 10% existing equations or laws, 80% data, and 10% expert knowledge.

3.2. Modelled optimization objectives

The modelling of the five objectives following the proposed methodology is given in the sections below. The modelling was done using experimental and industrial data, part of which is confidential, and so values of some of the coefficients cannot be given here.

3.2.1. Casein concentration (dry basis) in the retentate fraction: Retentate concentration

Retentate concentration ($CD_{CN,r}$) is the ratio of casein concentration in retentate ($C_{CN,r}$) to retentate dry matter (DM_r) (Eq. (2)). Casein concentration in the retentate fraction depends on the casein concentration in the feed milk ($C_{CN,milk}$) and the volume reduction ratio (VRR). Retentate dry matter is a function of casein concentration in the retentate fraction ($C_{CN,r}$) and the serum protein transmission rate at each stage (n) of the MF process ($TrSP_n$). $TrSP_n$, TMP, and hydraulic resistance of the fouled membrane (R_1) are dependent on type of membrane, and

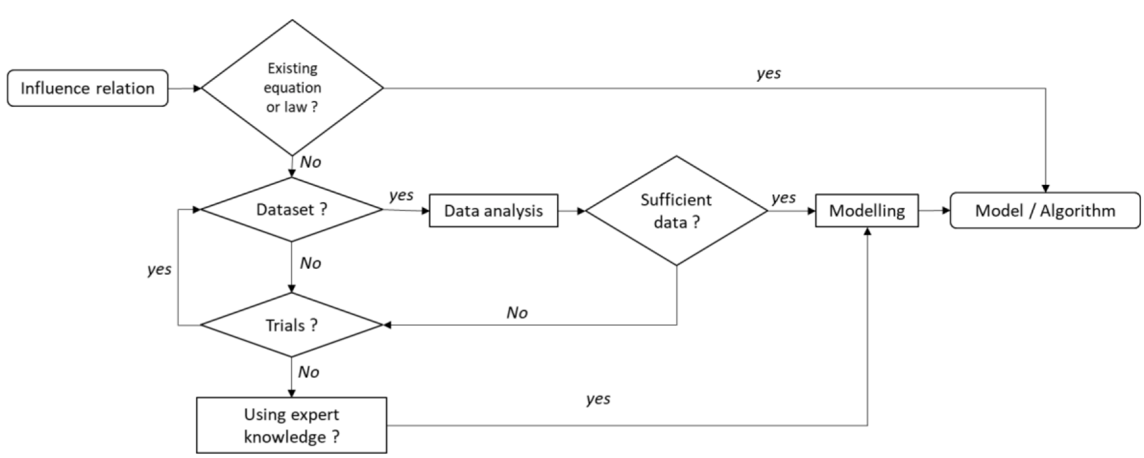

Fig. 1. Strategy for modelling MF objectives on product specifications.

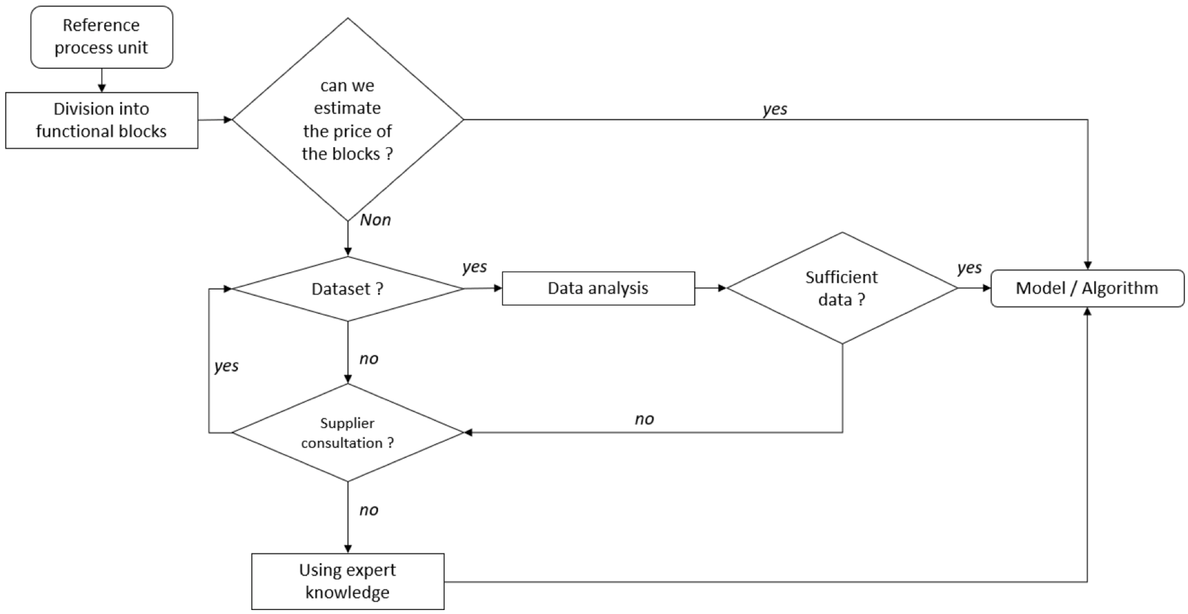

Fig. 2. Strategy for the modelling of MF objectives on economic costs.

their ranges reflect industry-practice reality.

$$CD_{CN,r} = \frac{C_{CN,r}}{DM_r} = \frac{VRR \bullet C_{CN,milk}}{a + b \bullet C_{CN,r} - c \bullet \frac{\sum_{k=1}^{n}\left(d - e \bullet VRR_k - f \bullet \left(Jp_1 \bullet \mu_p \bullet (g \bullet VRR_1 - h \bullet Q_{rec1})\right) - i \bullet Q_{rec}\right)}{n}} \; for\ 0 < n \leq 5 \tag{2}$$

Subject to.

$$VRR = \begin{cases} VRR_1\ if\ n = 1\ with\ 1 < VRR_1 \leq 3 \\ VRR_2\ if\ n = 2\ with\ 1 < VRR_1 < VRR_2 \leq 3 \\ VRR_3\ if\ n = 3\ with\ 1 < VRR_1 < VRR_2 < VRR_3 \leq 3 \\ VRR_4\ if\ n = 4\ with\ 1 < VRR_1 < VRR_2 < VRR_3 < VRR_4 \leq 3 \\ VRR_5\ if\ n = 5\ with\ 1 < VRR_1 < VRR_2 < VRR_3 < VRR_4 < VRR_5 \leq 3 \end{cases} \tag{3}$$

$$41.55 < C_{CN,r} < 105.26 \tag{4}$$

$$105.47 < DM_r < 174.15 \tag{5}$$

$$T = \begin{cases} 12\ if\ MT = SW \\ 50\ otherwise \end{cases} \tag{6}$$

$$\begin{cases} 0.016 < TrSP_k < 0.65\ if\ MT = SW \\ 0.43 < TrSP_k < 0.78\ if\ MT = GP \\ 0.34 < TrSP_k < 0.82\ if\ MT = UTP \end{cases} \tag{7}$$

$$\begin{cases} 0.48 < TMP < 1.25\ if\ MT = SW \\ 0.8 < TMP < 1.4\ if\ MT = GP \\ 0.31 < TMP < 0.6\ if\ MT = UTP \end{cases} \tag{8}$$

$$\begin{cases} 12 < Qrec < 21\ if\ MT = SW \\ 37 < Qrec < 43\ otherwise \end{cases} \tag{9}$$

$$\mu_p = \begin{cases} 1.73E-3\ if\ MT = SW \\ 6.48E-4\ otherwise \end{cases} \tag{10}$$

$$\begin{cases} 8.12E12 < R_1 < 5.94E13\ if\ MT = SW \\ 5.93E12 < R_1 < 1.78E13\ if\ MT = GP \\ 2.64E12 < R_1 < 1.07E13\ if\ MT = UTP \end{cases} \tag{11}$$

where

Jp_1 is permeation flux at stage 1, μ_p is permeate viscosity, Q_{rec} is retentate recirculation flowrate, T is filtration temperature, MT is membrane type, and a to i are the equation coefficients.

3.2.2. Serum protein concentration (dry basis) in the permeate fraction: Permeate concentration

Permeate concentration ($CD_{SP,p}$) is expressed as a ratio of serum protein concentration in the permeate fraction ($C_{SP,p}$) to dry matter of the permeate fraction (DM_p). $C_{SP,p}$ is a function of $TrSP_n$, and dry matter of the permeate fraction is a function of serum protein concentration in the permeate fraction (Eq. (12)). $TrSP$ is influenced by type of membrane, which explains why the range of the variable is also membrane type dependent. In fact, transmission rate is higher with ceramic membranes (UTP and GP), and especially ceramic UTP, than for the polymeric SW membrane.

$$CD_{SP,p} = \frac{C_{SP,p}}{DM_p} = \frac{a \bullet \frac{\sum_{k=1}^{n}\left(d - e \bullet VRR_k - f \bullet \left(Jp_1 \bullet \mu_p \bullet (g \bullet VRR_1 - h \bullet Q_{rec1})\right) - i \bullet Q_{rec}\right)}{n}}{b + c \bullet C_{SP,p}} \; for\ 0 < n \leq 5 \tag{12}$$

Subject to.

$$\begin{cases} 0.016 < TrSP_k < 0.65 \ if \ MT = SW \\ 0.43 < TrSP_k < 0.78 \ if \ MT = GP \\ 0.34 < TrSP_k < 0.82 \ if \ MT = UTP \end{cases} \tag{13}$$

$$0.59 < C_{SP,p} < 5.56 \tag{14}$$

$$56.3262 < DM_p < 61.89 \tag{15}$$

where

VRR_k is volume reduction ratio at MF stage k, Jp_1 is permeation flux at MF stage 1, μ_p is permeate viscosity, Q_{rec} is retentate recirculation flowrate, and a to i are the equation coefficients.

3.2.3. Serum protein recovery ratio in permeate fraction (Permeate recovery)

The permeate recovery (η_p) is the ratio of the serum protein quantity in the permeate fraction ($q_{SP,p}$) over the serum protein quantity in the feed milk ($q_{SP,milk}$) (Eq. (16)). In the permeate fraction, the serum protein quantity is expressed as a function of the serum protein concentration ($C_{SP,p}$), the feed volume of milk to be filtered by the MF (V_{feed}), the volume reduction ratio (VRR) and the permeate density (ρ_p). In the feed milk, the serum protein quantity is expressed as the serum protein quantity in the feed milk ($C_{SP,milk}$), the volume of the produced permeate fraction (V_p) and the milk density (ρ_{milk}).

$$\eta_p = \frac{q_{SP,p}}{q_{SP,milk}} = \frac{C_{SP,p} \bullet \left(V_{feed} - \left(\frac{V_{feed}}{VRR}\right)\right) \bullet \rho_p}{C_{SPmilk} \bullet V_{feed} \bullet \rho_{milk}} \tag{16}$$

$$CO_{Stages} = \begin{cases} \left((CO_{EXM} + CO_{PE}) \bullet F_{enc} + \sum_{k=1}^{n} (d \bullet Q_{PE,k} + e)\right) \bullet R_{EASW} + CO_{membranes} \ if \ MT = SW \\ \left((CO_{EXM} + CO_{PE}) \bullet F_{enc} + \sum_{k=1}^{n} (f \bullet Q_{PE,k} + g)\right) \bullet R_{EA} + CO_{membranes} \ otherwise \end{cases} \tag{19}$$

$$CO_{membranes} = \begin{cases} \dfrac{\left[\left(\frac{1}{VRR_{k-1}} - \frac{1}{VRR_k}\right) \bullet \left((h + l \bullet TMP_1 + m \bullet n) - (o + p \bullet TMP_1 + q \bullet r) \bullet \log\left(\frac{1}{VRR_k}\right)\right)\right] \bullet 1000Q_{feed}}{A_{CSW}} \bullet CO_{CSW} \ if \ MT = SW \\ \dfrac{\left[\left(\frac{1}{VRR_{k-1}} - \frac{1}{VRR_k}\right) \bullet \left((h + l \bullet TMP_1 + m \bullet n) - (o + p \bullet TMP_1 + q \bullet r) \bullet \log\left(\frac{1}{VRR_k}\right)\right)\right] \bullet 1000Q_{feed}}{A_{CGP}} \bullet CO_{CGP} \ if \ MT = GP \\ \dfrac{\left[\left(\frac{1}{VRR_{k-1}} - \frac{1}{VRR_k}\right) \bullet \left((h + l \bullet TMP_1 + m \bullet n) - (o + p \bullet TMP_1 + q \bullet r) \bullet \log\left(\frac{1}{VRR_k}\right)\right)\right] \bullet 1000Q_{feed}}{A_{CUTP}} \bullet CO_{CUTP} \ otherwise \end{cases} \tag{20}$$

3.2.4. Investment cost

The investment cost (CI) was broken down into six costs corresponding to the investment costs of the different 'functional' blocks (Eq. (17)), i.e., the feed and retentate areas, MF stages, permeate area, cleaning and disinfection, downstream environment and upstream environment. The cost of feed and retentate areas ($CO_{f\&r}$) differs according to whether the membrane is polymeric or ceramic (Eq. (18)). It is made up of the process feed tank (CO_{CA}), the feed pump (CO_{PA}), and structural cost to take into account piping, valving and sensors. The cost of MF stages (CO_{Stages}) includes the cost of the on-stage retentate pump (CO_{PE}), the permeate circulation pump (for the ceramic UTP only), the cost of the exchanger used to hold a constant filtration temperature (CO_{EXM}), and a structural cost (piping, valving and sensors) depending on the retentate recirculation flow rate and the cost-to-buy of the membranes (Eq. (19)). The cost of the permeate area (CO_{resP}) is correlated with the number of permeate extraction networks (Eq. (21)). The number of networks depends on the geometrical arrangement of the modules on the MF stage (j_k), a constant that takes into account piping, valving and sensors and a pump in the case of polymeric SW (CO_{PP}). In this specific case, the pump is used to prevent retrofiltration which can damage the polymeric membrane. The cost of the cleaning and disinfection area (CO_{MC}) is considered constant regardless of the type of membrane. The cost of the downstream area (CO_{down}) includes the cost of all necessary milk processing equipment, i.e., a storage tank (CO_{Cdown}), a heat exchanger to bring the milk to filtration temperature (CO_{EXdown}), an exchanger to hold the milk at filtration temperature for 20 min in order to reach physical–chemical equilibria (CO_{hold}), a transfer pump (CO_{PA}), and fixed costs corresponding to piping, valving and sensors (FF_{Am}) (Eq. (24)). The cost of the upstream area (CO_{up}) includes the cost of the equipment necessary for storing the permeate and retentate fractions obtained from the MF (Eq. (25)). Storage of the two fractions requires a tank (CO_{CP}, CO_{CR}) and a cooler (CO_{RP}, CO_{RR}), and also involves fixed costs corresponding to piping, valving and sensors (FF_{up}).

$$CI = CO_{f\&r} + CO_{Stages} + CO_{resP} + CO_{MC} + CO_{down} + CO_{up} \tag{17}$$

With.

$$CO_{f\&r} = \begin{cases} (a + b \bullet Q_{PA} + CO_{PA} \bullet F_{enc}) \bullet R_{EASW} + CO_{CA} \bullet F_{enc} \ if \ MT = SW \\ c \bullet R_{EA} + (CO_{CA} + CO_{PA}) \bullet F_{enc} \ otherwise \end{cases} \tag{18}$$

$$CO_{resP} = \begin{cases} s \bullet R_{EASW} \bullet max(j_k) + CO_{PP} \ if \ MT = SW \\ s \bullet R_{EA} \bullet max(j_k) \ otherwise \end{cases} \tag{21}$$

$$CO_{down} = CO_{Cdown} + CO_{EXdown} + CO_{PA} + FF_{down} + CO_{hold} \tag{22}$$

$$CO_{up} = \begin{cases} CO_{CP} + CO_{CR} + FF_{up} + CO_{RR} \ if \ MT = SW \\ CO_{CP} + CO_{CR} + FF_{up} + CO_{RR} + CO_{RP} \ otherwise \end{cases} \tag{23}$$

Subject to:

$$VRR_0 = 1 \tag{24}$$

where

VRR_0 is volume reduction ratio at MF stage 0, which is in fact the state of the feed with no concentration, Q_{PA} is feed pump flowrate, F_{enc} is cost of project management, R_{EASW} is automation ratio when using polymeric SW, R_{EA} is automation ratio when using ceramic GP or UTP, $Q_{PE,k}$ is pump flowrate on stage k, $CO_{membranes}$ is cost of the membranes, CO_{CSW} is cost of one module of polymeric SW, CO_{CGP} is cost of one module of ceramic GP, CO_{CUTP} is cost of one module of ceramic UTP, and a to s are equation coefficients.

3.2.5. Production cost

The production cost (CPR) is influenced by the cost of utilities such as electricity, water and vapor (CO_{ut}) and the annual cost of maintenance ($CO_{mt/y}$) (Eq. (25)). Cost of maintenance is expressed as: a ratio of investment cost to cost of membrane replacement according to type of membrane and their respective lifetime. This cost is calculated for two production runs and two cleaning operations per day for ceramic UTP and GP and one production run and one cleaning operations per day for polymeric SW.

$$CPR = CO_{ut} + CO_{mt/y} = CO_{ut} + \left(RMT \bullet CI + \frac{CO_{membranes}}{MLT} \right) \tag{25}$$

Subject to.

$$MLT = \begin{cases} 2 \ if \ MT = SW \\ 10 \ otherwise \end{cases} \tag{26}$$

where

RMT is maintenance ratio (-), CI is investment cost (€), $CO_{membranes}$ is membrane cost (€) and MLT is membrane lifetime (yr).

The objective functions reflect the assumptions and choices that determine the framework of the study. The solution space of the optimization is strongly constrained and restricted to the validity domains of the decision variables, where the ranges of variation of the polymeric membrane descriptors are wider than those for the ceramic membranes.

After modelling, several variables influence the same optimization objectives. The following example highlights the conflicting aspect of the microfiltration optimization objectives. The volume reduction ratio (VRR) influences the permeate recovery (n_p) and the production cost (CPR). The increasing of VRR increases the permeate recovery (Eq.29) as well as the $CO_{membrane}$ (Eq. (20)) and by the way the CPR; knowing that the permeate recovery is an objective to maximize while the production cost is an objective to minimize.

4. Skim milk microfiltration optimization

4.1. Multiobjective optimization

The MF multiobjective optimization problem can be summarized as:

$$maxCD_{CN,r} = max\left(\frac{VRR \bullet C_{CN,milk}}{a + b \bullet C_{CN,r} - c \bullet \frac{\sum_{k=1}^{n}\left(d - e \bullet VRR_k - f \bullet \left(Jp_1 \bullet \mu_p \bullet (g \bullet VRR_1 - h \bullet Q_{rec1})\right) - i \bullet Q_{rec}\right)}{n}} \right) \tag{27}$$

$$maxCD_{SP,p} = max\left(\frac{a \bullet \frac{\sum_{k=1}^{n}\left(d - e \bullet VRR_k - f \bullet \left(Jp_1 \bullet \mu_p \bullet (g \bullet VRR_1 - h \bullet Q_{rec1})\right) - i \bullet Q_{rec}\right)}{n}}{b + c \bullet C_{SP,p}} \right) \tag{28}$$

$$max\eta_p = max\left(\frac{C_{SP,p} \bullet \left(V_{feed} - \left(\frac{V_{feed}}{VRR}\right)\right) \bullet \rho_p}{C_{SPmilk} \bullet V_{feed} \bullet \rho_{milk}} \right) \tag{29}$$

$$minCI = min\left(CO_{f\&r} + CO_{Stages} + CO_{resP} + CO_{MC} + CO_{down} + CO_{up}\right) \tag{30}$$

$$minCPR = min\left(CO_{ut} + \left(RMT \bullet CI + \frac{CO_{membranes}}{MLT} \right) \right) \tag{31}$$

Subject to.

$$VRR = \begin{cases} VRR_1 \ if \ n = 1 \ with \ 1 < VRR_1 \leq 3 \\ VRR_2 \ if \ n = 2 \ with \ 1 < VRR_1 < VRR_2 \leq 3 \\ VRR_3 \ if \ n = 3 \ with \ 1 < VRR_1 < VRR_2 < VRR_3 \leq 3 \\ VRR_4 \ if \ n = 4 \ with \ 1 < VRR_1 < VRR_2 < VRR_3 < VRR_4 \leq 3 \\ VRR_5 \ if \ n = 5 \ with \ 1 < VRR_1 < VRR_2 < VRR_3 < VRR_4 < VRR_5 \leq 3 \end{cases} \tag{32}$$

$$41.55 < C_{CN,r} < 105.26 \tag{33}$$

$$105.47 < DM_r < 174.15 \tag{34}$$

$$T = \begin{cases} 12 \ if \ MT = SW \\ 50 \ otherwise \end{cases} \tag{35}$$

$$\begin{cases} 0.016 < TrSP_k < 0.65 \ if \ MT = SW \\ 0.43 < TrSP_k < 0.78 \ if \ MT = GP \\ 0.34 < TrSP_k < 0.82 \ if \ MT = UTP \end{cases} \tag{36}$$

$$\begin{cases} 0.48 < TMP < 1.25 \ if \ MT = SW \\ 0.8 < TMP < 1.4 \ if \ MT = GP \\ 0.31 < TMP < 0.6 \ if \ MT = UTP \end{cases} \tag{37}$$

$$\begin{cases} 12 < Qrec < 21 \ if \ MT = SW \\ 37 < Qrec < 43 \ otherwise \end{cases} \tag{38}$$

$$\mu_p = \begin{cases} 1.73E-3 \ if \ MT = SW \\ 6.48E-4 \ otherwise \end{cases} \tag{39}$$

$$\begin{cases} 8.12E12 < R_1 < 5.94E13 \ if \ MT = SW \\ 5.93E12 < R_1 < 1.78E13 \ if \ MT = GP \\ 2.64E12 < R_1 < 1.07E13 \ if \ MT = UTP \end{cases} \tag{40}$$

$$0.59 < C_{SP,p} < 5.56 \tag{41}$$

$$56.3262 < DM_p < 61.89 \tag{42}$$

$$VRR_0 = 1 \tag{43}$$

$$MLT = \begin{cases} 2 \ if \ MT = SW \\ 10 \ otherwise \end{cases} \tag{44}$$

The multiobjective optimization was done by NSGA-II using the Pymoo framework (Blank & Deb, 2020) implemented as per Deb et al. (2002). Population size was set to 1000 and offspring size was set to 2500. Distribution parameter was set to 30 and crossover and mutation operators were set to probabilities of occurrence of 0.9 and 0.5,

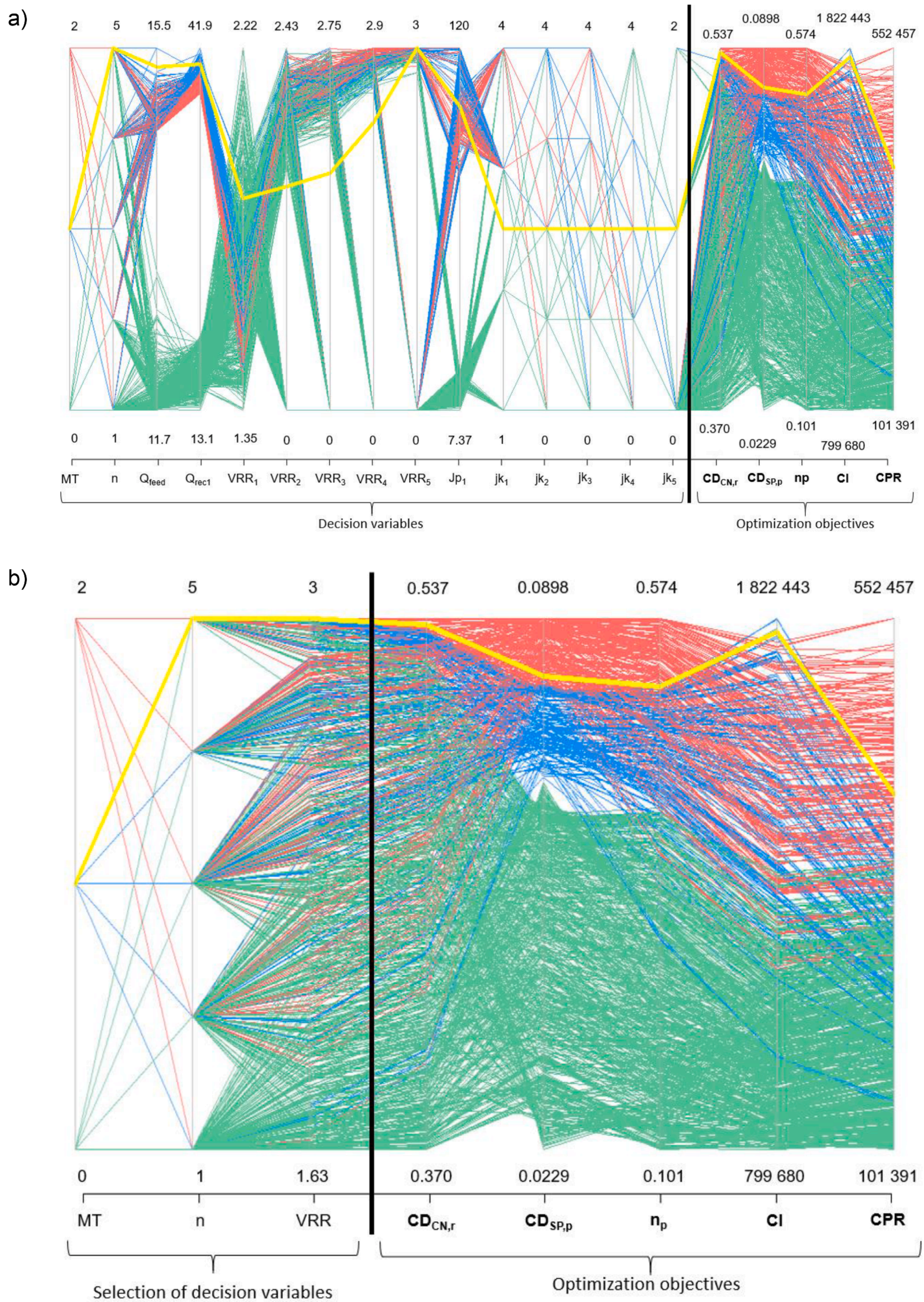

Fig. 3. (a) Parallel coordinates plot of the Pareto-optimal solutions found by NSGA-II multiobjective optimization of the MF process, with the decision variables on the left side of the vertical line, and the optimization objectives in bold on the right side of the vertical line. (b) A zoomed-in view of the parallel coordinates plot on the 3 main decision variables, showing the type of membrane (*MT*), number of MF stages (*n*) and volume reduction factor of the MF process (*VRR*) with the optimization objectives in bold. Three colours were used to highlight the types of membrane used in each Pareto-optimal solution: green for polymeric SW, blue for ceramic GP, and red for ceramic UTP. The yellow line represents the industrial process. (For interpretation of the references to colour in this figure legend, the reader is referred to the web version of this article.)

respectively. Tolerances on decision variables, objective functions and constraint values were set to 0.1, 0.01 and 0 (strict compliance), respectively. To simplify the modelling process, all the decision variables were set the same tolerance based on the limitation due to the measurement on the *VRR*. The same approach was used for the tolerance on the objective values and the limitation was set according to dry-basis serum protein concentration ($CD_{SP,p}$). All the parameters were set up after preliminary tests. The termination criterion was the maximum number of evaluations, which was set to 5,000,000. Milk volume treated per day (V_{feed}) was set to 230 m^3 and the milk and permeate compositions corresponded to typical average values i.e. casein concentration in milk, $C_{CN,milk} = 27$ g.kg^{-1} and serum protein concentration in milk, $C_{SP,milk} = 6.32$ g.kg^{-1}. Permeate density (ρ_p) was 990 kg.m^{-3} and milk density (ρ_{milk}) was 1032 kg.m^{-3}.

4.2. Optimization results and discussion

4.2.1. Overall results

The multiobjective optimization of 0.1-μm skim milk MF resulted in over 1000 Pareto-optimal solutions. A parallel coordinates plot of the Pareto-optimal solutions is given in Fig. 3a.

Polymeric SW membranes represented 58.8% of all the Pareto-optimal solutions, followed by ceramic UTP at 24.5% and ceramic GP at 16.7%. The solution space of the optimization, which was restricted to the validity domains of the decision variables, is less constrained for polymeric membranes than for ceramic membranes: ranges of variation of the decision variables (e.g. *TMP*, Q_{rec}) were larger for polymeric membranes than for ceramic membranes. This presupposes a greater number of possible configurations and potentially a greater number of Pareto-optimal solutions for polymeric SW.

When considering number of MF-system stages (*n*), Pareto-optimal solutions with 1, 2 or 3 MF stages represented 70% of all solutions, and the remaining 30% was represented by solutions with 4 or 5 MF stages (Fig. 3a and 3b). Note that Pareto-optimal solutions with a small number of MF stages (i.e., 1, 2 or 3) were unable to achieve a VRR higher than 2.75 and consequently a high casein concentration in the retentate fraction. These results are consistent with industrial installations, which tend to use 4 or 5 solutions when high concentration values are desired (VRR $\geq$ 3.0). This distribution of solutions according to number of MF stages can be explained by the sharp evolution in the rheological properties of casein concentrates as a function of concentration (and VRR): in the range of VRR between 3.0 and 3.5, the rheological behaviour of casein micelle concentrates changes drastically to become non-Newtonian, which results in strong drops in permeation flux. According to the principle of minimizing membrane area (Jeantet et al., 2011), the drop in flux leads to a higher theoretical number of MF stages.

This study thus highlights that solutions employing a low number of stages may represent interesting alternatives provided there is no need to strongly concentrate the caseins in the retentate and exceed a VRR of 3.0. The solutions proposed satisfy the goal of minimizing the cost, because a higher number of stages requires higher investment which thus leads to higher production costs. Therefore, the difference observed between the solutions proposed in this study, which have 3 or less stages, and a conventional plant configuration may come from the limitation used here on the *VRR* model ($1.0 < VRR \leq 3.0$), as the drastic change in rheological behaviour of the casein micelle concentrates when VRR greater than 3.0 results in strong drops in permeation flux and thus leads to a higher number of MF stages. The fact that a majority of Pareto-optimal solutions used a small number of stages may be explained by the fact that a lower number of stages requires a lower investment cost. Note that most of the data used for the design were obtained at constant permeation flux (*Jp*) and not at constant *TMP*, which can also lead to imprecision in establishing the sizing equation and, from there, in calculating the number of stages.

The values for feed flowrate of the MF system (Q_{feed}) clustered around two typical values, i.e., 12 m^3.h^{-1} for polymeric membranes and 14.5 m^3.h^{-1} for ceramic membranes. These values are consistent with what is observed in industry practice in the same feed conditions.

Q_{rec} values were not homogeneously distributed but fell into two typical ranges of values, i.e., 12–20 m^3.h^{-1} and 37–43 m^3.h^{-1}, which correspond to classical values for polymeric and ceramic membranes respectively (Gésan-Guiziou et al., 1999; Jimenez-Lopez et al., 2008; Zulewska & Barbano, 2013).

Permeation flux (*Jp*) also fell into two ranges of values, i.e., 5–20 L.h^{-1}.m^{-2} and 75–120 L.h^{-1}.m^{-2}, which again correspond to classical values for polymeric SW and ceramic membranes, respectively (Zulewska et al. 2009).

The values for the index of module position on MF stage k, *jk*, on each line *ik* were homogeneously distributed among their respective ranges regardless of membrane type (*MT*), which thus resulted in a large number of different combinations represented. As it is only a geometrical index, this decision variable influences the sizing of the retentate recirculation pump but does not have a significant influence on the optimization objectives.

To facilitate readability, (Fig. 3b) gives a zoom-in on the Pareto-optimal solutions based on three significant decision variables (type of membrane (*MT*), number of MF stages (*n*), and volume reduction factor of the global MF process (*VRR*).

The optimization objective values (Fig. 3b) warrant several observations. Retentate concentration (CD_{CNr}) is consistent with the values found in the literature. Regardless of *MT*, the solutions were fairly homogeneously distributed between 0.37 and 0.54 g.kg^{-1} DM (dry matter) for a *VRR* of between 1.63 and 3.0, respectively. The upper bound of the retentate concentration, CD_{CNr}, (0.54 g.kg^{-1} DM) corresponds to the casein concentration in milk multiplied by the VRR of 3.0 in the case of this study where there are no product losses.

Ceramic membranes, and particularly ceramic UTP, give higher permeate concentration (CD_{SPp}) and permeate recovery (n_p) values than polymeric membranes. The three membrane types cover different ranges of permeate concentrations with very little overlap, i.e., ceramic UTP 0.08–0.09 g.kg^{-1} DM, ceramic GP 0.06–0.08 g.kg^{-1} DM, and polymeric SW 0.02–0.06 g.kg^{-1} DM. As an example, the CD_{SPp} observed for ceramic UTP is greater than 0.08 g.kg^{-1} DM which corresponds to a C_{SPp} greater than 4.94 g.kg^{-1} and a n_p greater than 0.5. These permeate concentration and permeate recovery values are routinely found in industry practice with ceramic membranes. For illustrative comparison, the CD_{SPp} observed for polymeric membranes was lower than 0.07 g.kg^{-1} DM which corresponds to a C_{SPp} lower than 4.2 g.kg^{-1} and a n_p lower than 0.45. The ceramic GP gave CD_{SPp} and n_p values that were intermediate between ceramic UTP and polymeric SW membranes. This last observation was already highlighted in Mercier-Bouchard et al. (2017) and Tremblay-Marchand et al. (2016) but on limited ranges of operating conditions.

Analysis of the investment cost (*CI*) and production cost (*CPR*) found that solutions using ceramic membranes were logically more expensive than solutions with polymeric membranes (Fig. 3b), as ceramic membranes cost more i) in investment (€1 million–€2.5 million for ceramic *vs* €800,000–€1.8 million for polymeric) and ii) in production (€150,000–€800,000/year for ceramic *vs* €102,000–€553,000/year for polymeric membranes. This can be explained by the added permeate pump required to use the ceramic UTP and the high investment cost required to specifically manufacture the ceramic GP to get controlled variable permeability properties throughout the length of the filtering path. The surprising finding was Pareto-optimal solutions with a higher *CI* for ceramic GP than ceramic UTP. Indeed, even if the ceramic membrane does not need an additional pump, it still has a slightly higher *CI* than ceramic UTP membranes (Table 3). Consequently, for MF systems equipped with a large number of membranes, the investment cost will be higher with GP than UTP membranes.

These results confirm the existence of compromises in the choice of MF membrane type, operating conditions, and design to obtain the process that best meets end-user requirements. Indeed, polymeric

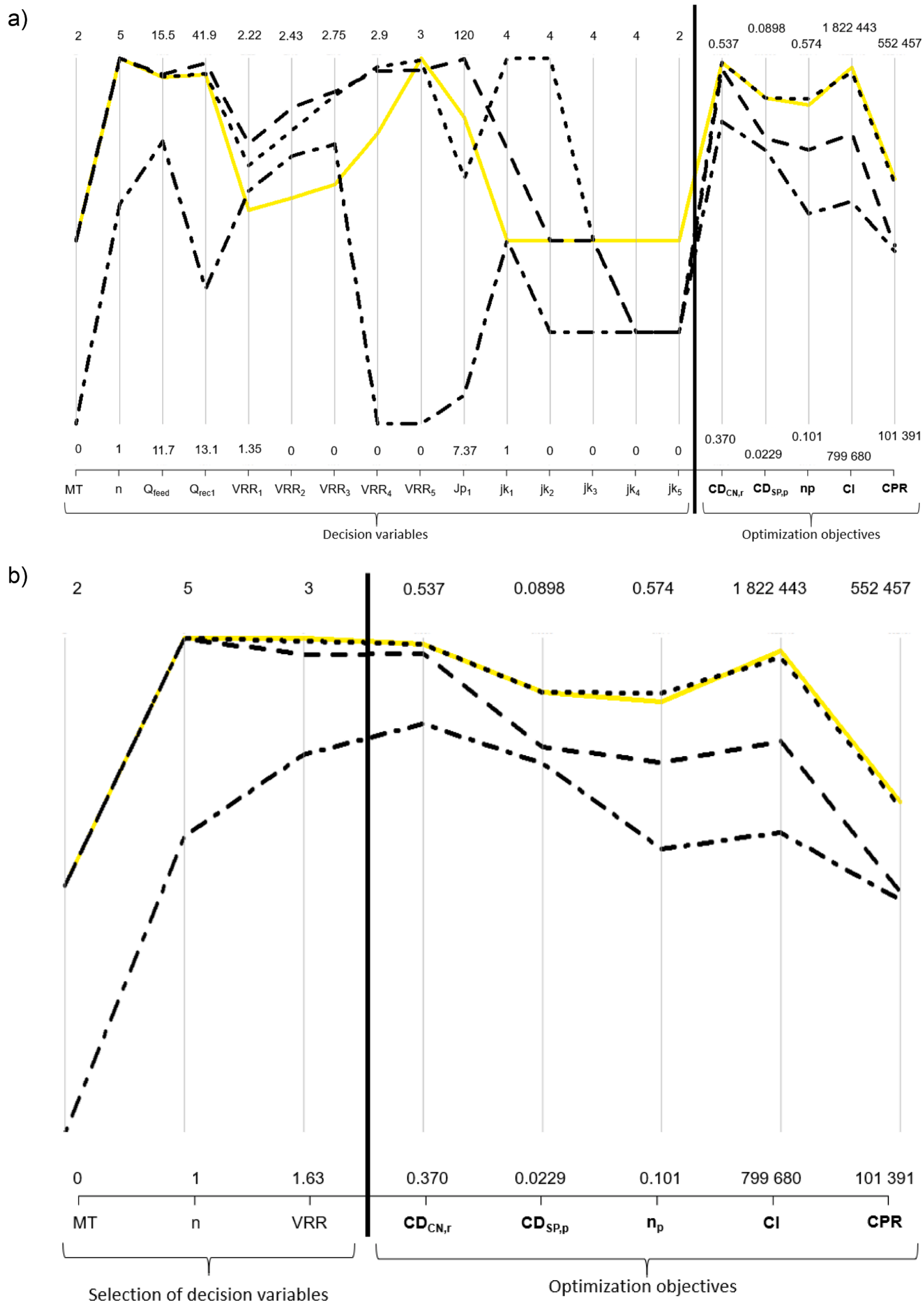

Fig. 4. (a) Parallel coordinates plot of the Pareto-optimal solutions found by NSGA-II multiobjective optimization of the MF process, with the decision variables on the left side of the vertical line, and the optimization objectives in bold on the right side of the vertical line. (b) A zoomed-in view of the parallel coordinates plot on the 3 main decision variables, showing the type of membrane (*MT*), number of MF stages (*n*) and volume reduction factor of the MF process (*VRR*) with the optimization objectives in bold. The yellow line represents the industrial process, the dotted line represents an equivalent Pareto-optimal solution, the dashed line represents a cheaper equivalent Pareto-optimal solution, and the dotted-and- dashed line represents an innovative Pareto-optimal solution. (For interpretation of the references to colour in this figure legend, the reader is referred to the web version of this article.)

Table 3
Decision variables used in the MF optimization problem and values of the objectives (in bold) for selected Pareto-optimal solutions (alternative solutions) compared to a standard industrial solution.

Decision variables/ Optimization objectives	Industrial process	Equivalent Pareto-optimal solution	Cheaper equivalent Pareto-optimal solution	Innovative Pareto-optimal solution
MT	1 (GP)	1 (GP)	1 (GP)	0 (SW)
Q_{feed} ($m^3.h^{-1}$)	14.71	14.74	14.84	11.99
Q_{rec1} ($m^3.h^{-1}$)	40.01	40.08	41.32	15.47
n	5	5	5	3
Jp_1 ($L.h^{-1}.m^{-2}$)	100.63	80.60	119.67	9.24
VRR_1	1.3	1.57	1.7	1.41
VRR_2	1.5	1.95	2.1	1.78
VRR_3	1.8	2.47	2.5	2.11
VRR_4	2.3	2.83	2.8	–
VRR_5	3.0	2.98	2.9	–
jki_1	2	4	3	2
jki_2	2	4	2	1
jki_3	2	2	2	1
jki_4	2	1	1	–
jki_5	2	1	1	–
CD_{CNr} ($g.kg^{-1}$ DM)	0.53	0.53	0.52	0.44
CD_{SPp} ($g.kg^{-1}$ DM)	0.08	0.08	0.07	0.07
n_p	0.50	0.51	0.43	0.33
CI (€)	1 774 431	1 751 361	1 443 187	1 108 872
CPR (€)	370 162	363 972	269 114	260 234

Table 4
Distribution of the membrane surface over the sequential MF stages.

Membrane surface (m^2)	Industrial process	Equivalent Pareto-optimal solution	Cheaper equivalent Pareto-optimal solution	Innovative Pareto-optimal solution
Stage 1	35.52	71.04	53.28	378.83
Stage 2	35.52	35.52	17.76	242.34
Stage 3	35.52	35.52	17.76	162.11
Stage 4	35.52	17.76	8.88	–
Stage 5	35.52	8.88	8.88	–
Total surface	177.60	168.72	106.56	783.29

membranes do not offer the best performances in terms of serum protein concentration and recovery efficiency, but this is offset by their relatively low investment and production costs, which makes them competitive with ceramic membranes. These factors which emerge from the global analysis of optimization solutions, support the current expert knowledge and literature in terms of design and performances in the field.

4.2.2. Analysis of particular Pareto-optimal solutions

In the Pareto front of solutions, there is a solution close to what is usually found in the dairy industry. Industrial facilities are generally designed with identical MF stage filtration areas with the same number of membranes, the same geometrical arrangement of the membranes, and the same operating conditions for each MF stage. Here we compare, a solution usually implemented at industrial scale, called "Industrial process" to three Pareto-optimal solutions: i) a solution equivalent to the one usually implemented at industrial scale, called "Equivalent Pareto-optimal solution"; ii) a solution equivalent to the industrial process but cheaper in terms of economic costs, called "Cheaper equivalent Pareto-optimal solution"; and iii) "An innovative Pareto-optimal solution involving polymeric membranes not commonly used at industrial scale" (Fig. 4). These solutions represent four MF facilities designed to process the same quantity of milk per day but with differences in design and performances.

Table 5
Operating conditions and filtration performances for standard industrial and alternative solutions.

Variable	Industrial process	Equivalent Pareto-optimal solution	Cheaper equivalent Pareto-optimal solution	Innovative Pareto-optimal solution
tf (h)	15.94	15.90	15.80	19.54
Q_{feed} ($m^3.h^{-1}$)	14.71	14.73	14.84	11.99
v ($m.s^{-1}$)	6.65	6.66	6.87	2.57
TMP (bar)	0.8	0.80	1.34	0.48
VRR1	1.3	1.57	1.7	1.41
Jp1 ($L.h^{-1}.m^{-2}$)	100.63	80.60	119.67	9.24
$TrSP_1$	0.70	0.69	0.59	0.56
VRR_2	1.5	1.95	2.1	1.78
Jp_2 ($L.h^{-1}.m^{-2}$)	62.57	60.85	80.77	7.25
$TrSP_2$	0.69	0.67	0.58	0.55
VRR_3	1.8	2.47	2.5	2.11
Jp_3 ($L.h^{-1}.m^{-2}$)	55.19	45.74	73.57	6.42
$TrSP_3$	0.68	0.66	0.57	0.53
VRR_4	2.3	2.83	2.8	–
Jp_4 ($L.h^{-1}.m^{-2}$)	48.69	39.11	70.51	–
$TrSP_4$	0.67	0.65	0.56	–
VRR_5	3.0	2.98	2.9	–
Jp_5 ($L.h^{-1}.m^{-2}$)	42.93	36.82	68.69	–
$TrSP_5$	0.65	0.64	0.56	–

Regarding the optimization objectives, the *Equivalent Pareto-optimal solution* gave similar values to the *Industrial process* working with the same membrane type (*MT*), number of MF stages (*n*) and volume reduction ratios (VRR_n) but a slightly different filtration area (A_k) and membrane surface distribution among the stages (jki_n) (see Table 3). There were no significant differences between *Industrial process* and *Equivalent Pareto-optimal solution* in terms of values of the optimization objectives, regardless of the objectives: all differences between values of objectives were less than 2%. However, the *Industrial process* was designed for a 177.6 m^2 membrane surface distributed evenly across the 5 MF stages whereas the *Equivalent Pareto-optimal solution* was designed for a 166.72 m^2 membrane surface that is not evenly distributed across the 5 MF stages (see Table 4). The *Industrial process* and the *Cheaper equivalent Pareto-optimal solution* were designed to have the same feed capacity (Q_{feed}) and to concentrate up to a volume reduction ratio of 3.0 (*VRR*). These solutions used similar values for retentate concentration ($CD_{CN,r} = 0.53$ $g.kg^{-1}$ DM) due to the protein concentrations processed up to the same volume reduction ratio ($VRR = 3.0$), and the same permeate concentration ($CD_{SP,p} = 0.08$ $g.kg^{-1}$ DM). However, permeate recovery (*np*) was lower in the *Cheaper equivalent Pareto-optimal solution* ($n_p = 0.43$), with a loss of 14% compared to the *Industrial process* ($n_p =$ 0.51). These differences in permeate recovery can be explained by the operating conditions (see Table 5) and especially by the higher *TMP* of the *Cheaper equivalent Pareto-optimal solution* (1.34 bar) than the *Industrial process* (0.80 bar). In terms of investment cost and production cost objectives, the *Cheaper equivalent Pareto-optimal solution* can save 19% and 27%, respectively, compared to the *Industrial process*. Indeed, the *Cheaper equivalent Pareto-optimal solution* was designed to use 106.56 m^2 of membrane surface unevenly distributed across 5 stages whereas the *Industrial process* was designed to use a 177.6 m^2 membrane surface distributed evenly across the 5 MF stages (see Table 4). The differences in the investment and production costs can be explained by both the distribution of the membrane surface on the stages of the unit and the associated operating conditions, especially *VRR* management of the MF stages (see Table 5). For the same membrane type, a smaller required surface means lower investment and production costs. The *Cheaper equivalent Pareto-optimal solution* emerged as a good candidate alternative in terms of four out of five optimization objectives, but the loss of permeate recovery points to issues in terms of whether the solution is viable in industrial-scale practice. In fact, when calculating the ratio of quantity of serum proteins in the permeate to cost of production, the *Cheaper equivalent Pareto-optimal* solution remains attractive at €400/kg against €470 €/kg for the *Industrial solution*. The *Innovative Pareto-optimal solution* was designed to work with a polymeric SW membrane of 783.29 m^2 surface area unevenly distributed across three MF stages (see Tables 3 and 4). A smaller VRR means a lower number of MF stages required. Here, VRR = 2.11 corresponds to a 3-MF-stage process, which thus leads to a lower casein concentration in the retentate ($CD_{CN,r}$ = 0.44 $g.kg^{-1}$ DM; see Table 3). This *Innovative Pareto-optimal solution* performed badly on permeate recovery ($n_p = 0.33$). However, the value of this solution is that a small (-16%) decrease in retentate concentration comes with a very significant decrease in investment cost (−37%) and production cost (−30%). This kind of solution can be used in industry practice for production requiring relatively low removal of serum protein from the retentate and a relatively low casein concentration.

The approach developed here makes it possible to propose Pareto-optimal solutions at lower cost and innovative MF processes that have never been implemented.

5. Conclusion

Here we proposed an innovative approach for optimizing 0.1-μm-membrane skim milk microfiltration, which is a complex food process, as a multiobjective problem. This new approach was made possible by combining and integrating different types of knowledge, by modelling the optimization problem objectives, and by the multiobjective optimization itself. The problem was formulated and solved by coupling the integration of expert and scientific knowledge with multiobjective problem theory. We considered 15 decision variables including type of membrane (polymeric SW, ceramic UTP and ceramic GP) to optimize five objectives (three technical objectives and two economic) using the well-known and now-classical NSGA-II metaheuristic algorithm. The optimization provided over 1000 Pareto-optimal solutions, including one that was close to a ‘standard’ industrial process and another that provided comparable results at lower economic cost. Among these Pareto-optimal solutions, 58.8% used a polymeric SW membrane, 24.5% used a ceramic UTP membrane and 16.7% used a ceramic GP membrane. The computational Pareto-optimal solutions offer alternative and potentially innovative process pathways that need to be validated in order to assess their feasibility at industrial scale.

This work shows that coupling the integration of expert and scientific knowledge with multiobjective optimization is a successful method for modelling the multiobjective problem of skim milk microfiltration and more generally of any food processes that have not been scientifically characterized. These computational approaches helped us to think outside the box of classical MF process design schemes, to re-evaluate *a priori* unattractive technical solutions or scientifically validate new ones, even if huge number of Pareto-optimal solutions found make it not humanly feasible to choose the single preferred solution, even for an expert. To address this last difficulty, an additional multicriteria decision support step will be necessary to guide the decisionmaker through the process of selecting one or more preferred solutions from among a vast set of Pareto-optimal solutions.

CRediT authorship contribution statement

Maëllis Belna: Conceptualization, Methodology, Software, Validation, Data curation, Formal analysis, Writing – original draft, Writing – review & editing. **Amadou Ndiaye:** Conceptualization, Methodology, Validation, Supervision, Writing – review & editing. **Franck Taillandier:** Conceptualization, Methodology, Validation, Supervision, Writing – review & editing. **Christophe Fernandez:** Software. **Louis Agabriel:** Software, Supervision, Funding acquisition. **Geneviève Gésan-Guiziou:** Conceptualization, Validation, Supervision, Writing – review & editing, Funding acquisition.

Declaration of Competing Interest

The authors declare that they have no known competing financial interests or personal relationships that could have appeared to influence the work reported in this paper.

Acknowledgements

This study was supported by a grant from the Brittany Region (contract no. 16006734, INRAE funding agreement 30001292) and from the European Regional Development Fund (FEDER contract no. EU000171, INRAE funding agreement 30001293). The authors thank all the members of the project group.

References

Amiryousefi, M. R., Mohebbi, M., Khodaiyan, F., & Ahsaee, M. G. (2014). Multi-objective optimization of deep-fat frying of ostrich meat plates using multi-objective particle swarm optimization (MOPSO). *Journal of Food Processing and Preservation, 38*, 1472–1479.

Baudrit, C., Sicard, M., Wuillemin, P. H., & Perrot, N. (2010). Towards a global modelling of the Camembert-type cheese ripening process by coupling heterogeneous knowledge with dynamic Bayesian networks. *Journal of Food Engineering, 98*(3), 283–293.

Beckman, S. L., & Barbano, D. M. (2013). Effect of microfiltration concentration factor on serum protein removal from skim milk using spiral-wound polymeric membranes. *Journal of Dairy Science, 96*(10), 6199–6212.

Belna, M., Ndiaye, A., Taillandier, F., Agabriel, L., Marie, A. L., & Gésan-Guiziou, G. (2020). Formulating multiobjective optimization of 0.1 μm microfiltration of skim milk. *Food and Bioproducts Processing, 124*, 244–257.

Blank, J., & Deb, K. (2020). Multi-objective optimization in Python. *IEEE Access, 8*, 89497–89509.

Brans, G. B. P. W., Schroën, C. G. P. H., Van der Sman, R. G. M., & Boom, R. M. (2004). Membrane fractionation of milk: State of the art and challenges. *Journal of Membrane Science, 243*(1–2), 263–272.

Cooke, N. J. (1994). Varieties of knowledge elicitation techniques. *International Journal of Human Studies, 41*(6), 801–849.

Deb, K. (1999). Multi-objective genetic algorithms: Problem difficulties and construction of test problems. *Evolutionary Computation, 7*(3), 205–230.

Deb, K., Pratap, A., Agarwal, S., & Meyarivan, T. (2002). A fast and elitist multiobjective genetic algorithm: NSGA-II. *IEEE Transactions on Evolutionary Computation, 6*(2), 182–197.

Deka, D., & Datta, D. (2017). Multi-objective optimization of the scheduling of a heat exchanger network under milk fouling. *Knowledge-Based Systems, 121*(C), 71–82.

Garcera, D., Toujas, E., 1998. Macroporous support with permeability gradient and it manufacturing process. 0870534A1 [FR 9704359].

Gésan-Guiziou, G., Boyaval, E., & Daufin, G. (1999). Critical stability conditions in crossflow microfiltration of skimmed milk: Transition to irreversible deposition. *Journal of Membrane Science, 158*, 211–222.

Hartinger, M., & Kulozik, U. (2020). Milk protein fractionation by spiral-wound microfiltration membranes in diafiltration mode - Influence of feed protein concentration and composition on the filtration performance. *International Dairy Journal, 102*, 104606.

Heidebrecht, H.-J., Toro-Sierra, J., & Kulozik, U. (2018). Concentration of immunoglobulins in microfiltration permeates of skim milk: Impact of transmembrane pressure and temperature on the IgG transmission using different ceramic membrane types and pore sizes. *Foods, 7*(7), 101.

Hobballah, M. H., Ndiaye, A., Michaud, F., & Irle, M. (2018). Formulating preliminary design optimization problems using expert knowledge: Application to wood-based insulating materials. *Expert Systems with Applications, 92*, 95–105.

Hwang, C.-L., Masud, A.S.M. (1979). Multiple Objective Decision Making — Methods and Applications: A State-of-the-Art Survey. Lecture Notes in Economics and Mathematical Systems, Pages 12-20. Springer-Verlag, Berlin.

Janaszek-Mankowska, R. W. (2018). Multi-objective optimization of the apple drying and rehydration processes parameters. *Emirates Journal of Food and Agriculture, 30*(1), 1–9.

Jeantet, R., Roignant, M., & Delaplace, G. (2011). *Génie des procédés appliqué à l'industrie laitière*. Paris: Editions Tec & Doc.

Jimenez-Lopez, A., Leconte, N., Dehainault, O., Geneste, C., Fromont, L., & Gésan-Guiziou, G. (2008). Role of milk constituents on critical conditions and deposit

structure in skim milk microfiltration (0.1μm). *Separation and Purification Technology, 61*, 33–43.
Kennedy, J., Eberhart, R. (1995). Particle swarm optimization, in: Proceedings of ICNN'95 - International Conference on Neural Networks, *4*, 1942–1948.
Lawrence, N. D., Kentish, S. E., O'Connor, A. J., Barber, A. R., & Stevens, G. W. (2008). Microfiltration of skim milk using polymeric membranes for casein concentrate manufacture. *Separation and Purification Technology, 60*, 237–244.
Le Berre, O., & Daufin, G. (1996). Skimmilk crossflow microfiltration performance versus permeation flux to wall shear stress ratio. *Journal of Membrane Science, 117*, 261–270.
Mercier-Bouchard, D., Benoit, S., Doyen, A., Britten, M., & Pouliot, Y. (2017). Process efficiency of casein separation from milk using polymeric spiral-wound microfiltration membranes. *Journal of Dairy Science, 100*(11), 8838–8848.
Milton, N. R. (2007). *Knowledge Acquisition in Practice*. A step-by-step Guide: Springer Publishing Company, Incorporated.
Montibeller, G., & Belton, V. (2006). Causal maps and the evaluation of decision options - a review. *Journal of the Operational Research Society, 57*(7), 779–791.
Ndiaye, A., Castéra, P., Fernandez, C., & Michaud, F. (2009b). Multi-objective preliminary ecodesign. *International Journal on Interactive Design and Manufacturing, 3* (4), 237–245.
Ndiaye, A., Della Valle, G., Roussel, P. (2009a). Qualitative modelling of a multi-step process: the case of French breadmaking. *Expert Systems with Applications*, *36*(2, Pt 1), 1020–1038.
Reyes-Sierra, M., & Coello Coello, C. (2006). Multi-objective particle swarm optimizers: A survey of the state-of-the-art. *International Journal of Computational Intelligence Research, 2*(3), 287–308.
Saboya, L. V., & Maubois, J. L. (2000). Current developments of microfiltration technology in the dairy industry. *Le Lait, 80*(6), 541–553.
Sandblöm, R.M. (1974). Filtering process. Swedish Patent N° 7.416.257.
Sicard, M., Baudrit, C., Leclerc-Perlat, M. N., Wuillemin, P. H., & Perrot, N. (2011). Expert knowledge integration to model complex food processes. Application on the camembert cheese ripening process. *Expert Systems with Applications, 38*(9), 11804–11812.
Skrzypek, M., & Burger, M. (2010). Isoflux® ceramic membranes — Practical experiences in dairy industry. *Desalination, 250*(3), 1095–1100.
Tolkach, A., & Kulozik, U. (2006). Transport of whey proteins through 0.1 μm ceramic membrane: Phenomena, modelling and consequences for concentration or diafiltration processes. *Desalination, 199*, 340–341.
Tremblay-Marchand, D., Doyen, A., Britten, M., & Pouliot, Y. (2016). A process efficiency assessment of serum protein removal from milk using ceramic graded permeability microfiltration membrane. *Journal of Dairy Science, 99*(7), 5230–5243.
Van Veldhuizen, D. A., & Lamont, G. B. (2000). Multiobjective evolutionary algorithms: Analyzing the state-of-the-art. *Evolutionary Computation, 8*(2), 125–147.
de Vitor, J. F. A., & da Gomes, M. M. R. C. (2011). Estimation of coefficients of fluidized bed drying through the PSO and GA metaheuristic approaches. *Drying Technology, 29* (7), 848–862.
Wolpert, D. H., & Macready, W. G. (1997). No free lunch theorems for optimization. *IEEE Transactions on Evolutionary Computation, 1*(1), 67–82.
Yusoff, Y., Ngadiman, M. S., & Zain, A. M. (2011). Overview of NSGA-II for optimizing machining process parameters. *Procedia Engineering, 15*, 3978–3983.
Zulewska, J., Newbold, M., & Barbano, D. M. (2009). Efficiency of serum protein removal from skim milk with ceramic and polymeric membranes at 50°C. *Journal of Dairy Science, 92*(4), 1361–1377.
Zulewska, J., & Barbano, M. (2013). Influence of casein on flux and passage of serum proteins during microfiltration using polymeric spiral-wound membranes at 50°C. *Journal of Dairy Science, 96*(4), 2048–2060.